

# FADE DURATION DISTRIBUTIONS DERIVED FROM THE ACTS RADIOMETER DATA

K.S. McCormick, Larus Technologies Corp., Ottawa, Canada

D.V. Rogers, Communications Research Centre Canada, Department of Industry, Ottawa, Canada

## ABSTRACT

One of the criteria defining the quality of a communications system is the probability of the system being unavailable for a given time period. It is therefore useful to determine not only the annual statistics of signal attenuation due to rain, but also the statistics of the rain fade durations. The huge ACTS database provides a unique opportunity to study the conditional statistics of the duration of fades exceeding different thresholds. Earlier studies at 12 GHz found that a double-exponential model of the conditional probability of fade duration gave excellent agreement with measured values, over fade durations ranging from two seconds to more than one hour, indicating that two distinct rain processes are involved. Analysis of the ACTS radiometer data at 20 and 27 GHz suggests that the distributions at these higher frequencies can usually be decomposed into three, and sometimes four, separate exponential distributions, with decay constants ranging from the order of hours to the order of seconds. The three longest times are tentatively associated with attenuation due to atmospheric gases and cloud, with stratiform rain, and with convective rain. It is also suggested that the shortest decay times may be associated with the antenna wetting problem experienced by the ACTS terminals.

## 1. INTRODUCTION

Increasing demand for satellite capacity to support new services has required the use of higher frequencies, i.e., the Ku (14/12 GHz) and Ka (30/20 GHz) bands, for which attenuation due to rain is one of the most critical factors in satellite link design. The reliability of satellite links can be improved by providing suitable compensation techniques such as fade countermeasures and site diversity. Challenging questions in satellite system design are how much link margin is sufficient and what if any compensation schemes should be provided, given economic constraints. Rain attenuation statistics, both long-term (e.g., annual cumulative) and short-term (e.g., fade-duration), are important factors. For example, statistics for fades of greater than 10-sec duration are needed to meet ITU-T design requirements for high-quality data transmission services, since Recommendations ITU-T G.821 [1] and G.826 [2] define unavailable time as that where a link outage ( $BER < 10^{-3}$ ) occurs for more than 10 consecutive seconds.

In a study of 20-GHz Olympus data taken at Eindhoven, The Netherlands, Brussaard [3] showed that the conditional exponential distribution provided a model for the probability of long outages due to rain. With 12-GHz radiometer data from Southeast Asia [4], later studies [5] found that a double-exponential model of the conditional probability of fade duration gave excellent agreement with measured values for fade durations ranging from two seconds to more than one hour, indicating that two distinct rain processes were involved. This paper presents fade duration statistics derived from the 20- and 27-GHz radiometric measurements from the ACTS propagation experiments. Analysis of these data indicates that the fade distributions can generally be decomposed into three, and sometimes four, separate exponential distributions, with decay constants ranging from the order of seconds to the order of hours. The three longest times are tentatively associated with attenuation due to atmospheric gases and cloud, with stratiform rain, and with convective rain, respectively. It is suggested that the shortest decay times may be associated with the antenna wetting effects experienced by the ACTS terminals [6],[7].

## 2. DATA ANALYSIS

Statistics of fade duration are normally presented as conditional probabilities, i.e., the probability of a fade exceeding a certain duration, given that the fade depth has exceeded a specified threshold. In computing such statistics from measurements of satellite beacon signal level, a severe problem is that the recorded signal varies due to nonprecipitation effects, including receiver noise, tropospheric scintillations and nonrain fading. Some form of low-pass filtering is required to deal with periods where the signal may fluctuate around a threshold, creating a large number of short-duration fade events that are not due to rain. For example, Brussaard's analysis [3] only considered fade durations greater than 60 seconds. He first conditioned his data with a low-pass filter with a cutoff frequency of 0.02 Hz, then applied the condition that a threshold duration (of more than 60 seconds) was considered to have ended only if the threshold level was not exceeded again within 60 seconds of the stop time. The use of radiometer data to compute fade duration statistics removes this difficulty since nonprecipitation events other than low-level, relatively slow gaseous absorption, do not affect the radiometric skynoise temperature.

In the present study, attenuations inferred from the radiometer data were extracted from the archived, preprocessed ACTS data files. The radiometers were calibrated each 15 minutes, causing a loss of data for about 25 seconds. Since continuous records are essential for the determination of duration statistics, it was decided to automatically carry out a linear interpolation across any period of missing attenuation values, provided that the period did not exceed 30 seconds. Periods of data loss exceeding 30 seconds were dealt with during a manual editing process, which also removed most minor problems that survived the preprocessing. Again, linear interpolation across bad or missing data was used unless the problems were severe, in which case the data were simply deleted, one hour at a time.

At this stage, no attempts were made to remove the effects of attenuation due to atmospheric gases, or of signal losses related to antenna wetting, although both effects are amenable to correction [6],[7].

After the editing process, conditional fade duration distributions were calculated for fade thresholds of 2, 4, 6, 8 and 10 dB. From a visual examination of the data records, a hysteresis value of 0.2 dB was applied, i.e., a fade was not considered to have ended until the attenuation fell 0.2 dB below its threshold. This value appears, in most cases, sufficient to remove small residual noise in the data records.

In a previous study using 12-GHz attenuation data from Southeast Asia [4], fade distributions were found to be well described by a double-exponential function. Figure 1 shows a distribution for Bangkok, Thailand, for a fade threshold of 2 dB, along with the fitted function

$$P(d > D) = 0.591 \times \exp(-D/306) + (1 - 0.591) \times \exp(-D/2642) \quad (1)$$

The term  $(1-0.591)$  reveals that the fit was forced to go through probability  $P = 1$  for a fade duration  $d = 0$  sec. The constants 306 and 2642 are here called characteristic durations because they give a measure of the respective fade durations characteristic of each term of the equation. The first term was postulated to represent convective rain (shorter durations) and the second term, stratiform rain (longer durations).

Figure 2 shows a similar plot using 27-GHz data from the Oklahoma site, with data from three years combined to increase the stability of the statistics. Again, the fade threshold is 2 dB and a double-exponential fit is shown for the distribution. In this case the double-exponential is a poor fit to the data, showing a significant departure at the knee of the curve, and an inadequate representation of the tail of the curve, as well.

Because of the poor fit, a different strategy was attempted. First, the tail of the curve was examined, and a portion of the tail that appeared straight on a log plot was selected. In Figure 2, this range is shown as a thicker line. Next, an exponential fit was applied to the data in this range, resulting in the equation

$$P_1(d > D) = 0.293 \times \exp(-D/3574) \quad (2)$$

This function was then subtracted from the original data, resulting in the curve labeled "Curve fit 2" in Figure 3. Again, a linear range in the tail of this curve was selected as shown by the thickened portion of the curve, and a new exponential fit found:

$$P_2(d > D) = 0.288 \times \exp(-D/478) \quad (3)$$

It was possible to repeat the process two more times, as shown in Figure 4, resulting in the equations 4 and 5:

$$P_3(d > D) = 0.317 \times \exp(-D/63.7) \quad (4)$$

$$P_4(d > D) = 0.124 \times \exp(-D/18.9) \quad (5)$$

These equations show some interesting characteristics. First, for each fitting process, there does not appear to be any significant part of the tail left over after a function is subtracted. (It seems reasonable to ignore resulting data that occur with a probability less than 0.01.) This result implies that there are no "cross" terms between the distributions and that they are therefore statistically independent. Second, the selections of the straight portions of the curve tails were made entirely by eye; no constraints were placed on the selections. The sum of the coefficients in equations (2) through (5) gives a value of 1.022, differing by only 2 percent from the expected value of unity. Thus it appears that the four equations account for the totality of the original probability curve with nothing added and nothing left over.

Table 1 gives the coefficients for the fits to all five fade thresholds for the Oklahoma 27 GHz data. Three exponential equations were derived at each fade threshold except the first, for which four equations were found.

Table 1. Coefficients of the exponential fits to the Oklahoma 27-GHz data

Threshold→	2 dB	4 dB	6 dB	8 dB	10 dB
Coeff. 1	0.293	0.347	0.279	0.358	0.361
Coeff. 2	0.288	0.245	0.384	0.281	0.377
Coeff. 3	0.317	0.411	0.325	0.349	0.273
Coeff. 4	0.124	-	-	-	-
<b>Sum:</b>	1.022	1.003	0.983	0.987	1.011

### 3. RESULTS

Data have been analyzed for the locations and years shown in the first column of Table 2 (a total of seven station-years). Table 2 is intended to act as a guide to the 'goodness' of the analysis, according to the criterion that the coefficients of the exponential equations extracted from the distributions should sum to 1. Each cell corresponding to a given location and fade threshold shows first the sum of the coefficients and then, in brackets, the number of exponential equations derived for that case.

In the majority of cases, it is seen that the coefficients do, indeed, sum to a total close to 1, which lends credence to the analysis. Particular exceptions are in the BC data at fade thresholds of 2 and 8 dB, and in most instances of the MD analysis. All these cases need to be revisited, but it was noticed that the 20-GHz radiometer data for MD often showed rapid fluctuations of several tenths of a dB which appear to be equipment-related. It may be fruitful to apply a low-pass filter to these data.

The physical interpretation of the coefficients can be stated in the following manner. Consider the equation for Curve fit 2 in Figure 3. The coefficient in this equation is 0.298. If we associate this second curve with stratiform rain, we may say that, given that a 2-dB fade threshold has been exceeded, then the probability that this fade belongs to the stratiform-rain population is 0.298. The coefficient says nothing about the probability of occurrence of a 2-dB fade or the total duration of 2-dB fades.

Table 2. Sum of coefficients for data analyzed to date

Threshold→	2 dB	4 dB	6 dB	8 dB	10 dB
OK 95-97 20 GHz	0.965 (3)	0.986 (3)	1.034 (3)	1.021 (3)	1.032 (3)
OK 95-97 27 GHz	1.022 (4)	1.003 (3)	0.983 (3)	0.987 (3)	1.011 (3)
FL 97 20 GHz	1.024 (4)	0.947 (3)	0.996 (4)	0.903 (4)	0.893 (3)
FL 97 27 GHz	1.012 (4)	0.999 (3)	0.966 (3)	1.003 (3)	0.996 (4)
BC 96-97 20 GHz	0.871 (4)	0.930 (4)	1.139 (4)	0.714 (3)	1.001 (3)
BC 96-97 27 GHz	0.796 (4)	0.960 (4)	0.988 (4)	0.772 (3)	0.932 (3)
MD 97 20 GHz	1.058 (4)	1.275 (4)	1.341 (4)	1.248 (3)	1.180 (3)
MD 97 27 GHz	0.984 (3)	0.751 (3)	0.741 (4)	0.861 (2)	0.527 (3)

As a matter of interest, Table 3 shows the calculated number of fades and total fade durations at each fade threshold.

Table 3. Fade numbers and total durations for Oklahoma 1995-97

Fade Threshold	Number of Fades	Fade Seconds	Percent of Year
2	1712	1490769	1.57
4	1337	949720	1.00
6	1177	613869	0.65
8	940	404740	0.43
10	734	288701	0.30

Figure 5 shows the characteristic durations of the exponential equations plotted as a function of fade threshold, again for the Oklahoma 27-GHz attenuations. Also shown are exponential fits to the characteristic durations, and in this case the fits show excellent agreement. (No fit was possible for the shortest duration since only one point is available.) Because the fits are so good, they are considered as a reference points, and the three lines are therefore repeated in the next several figures.

Figure 6 shows the characteristic durations for the Oklahoma data at 20 GHz. The scatter is larger than in Figure 5, but the trends seem to be similar and no strong frequency dependence is obvious.

Figure 7 shows the Florida 1997 data at 20 and 27 GHz. The two longer durations are remarkably similar to the Oklahoma data. The 20-GHz durations may be somewhat smaller than those at 27 GHz, but again there does not appear to be a strong dependence.

Figure 8 presents the British Columbia 1996-97 data. As mentioned earlier, there may be problems with a few of the points, and the scatter is larger than in the previous cases, but the trend lines seem clearly flatter than for either Oklahoma or Florida. One explanation could involve the climate type, with British Columbia being a maritime rain climate and the other two having much more thunderstorm activity.

Figure 9 shows the Maryland 1997 analysis. The scatter in the points is quite large, and any trend lines may be somewhat flatter than the Oklahoma lines. The shortest duration points at the bottom of the graph may be informative. They were found only in the 20-GHz data, and it was in these data that there appeared to be some equipment instabilities.

Figure 10 compares the Oklahoma trend lines with other data that have been collected. The filled triangles with dashed lines show 12-GHz radiometer durations collected in Southeast Asia during 1992 to 1995. A total of 12 station-years are averaged in these points. The open triangles show data from a 12-GHz radiometer at Ottawa, for the period 1996 to 1998. Finally, the open squares give data from Europe using the Olympus beacon at 20 GHz, for long duration fades only. The Asian data, from a tropical rain climate characterized by substantial amounts of convective rainfall, show longer characteristic durations, as could be expected. The dashed lines should probably be compared with the lower two solid lines, and show less dependence on fade depth than the Oklahoma data. Interestingly, the European data for 20 GHz compare closely with the longer-duration Ottawa data at 12 GHz.

#### 4. CONCLUSIONS

Previous analyses of 12-GHz fade-duration statistics for Southeast Asian locations revealed a natural partition of the population into long and short durations, which appeared related to stratiform and convective rain regimes, respectively [5]. Results of the fade-duration analysis presented in this paper indicate that the overall patterns of signal fading behavior appear related to the distinct character of the fading introduced not only because of the climate type (tropical, maritime, continental) and characteristics of the fading process itself (e.g., distinct durations of fading induced by stratiform or cumulative rain), but perhaps to other apparent fade mechanisms that modulate the fading, such as equipment influences (antenna wetting) or even hardware faults. All of the features appear to be represented quite well by cascaded exponential fits to the distribution, and these distributions seem to represent independent phenomena. Therefore, the procedure appears capable of segmenting individual contributors to the overall fading distribution, and possibly of describing their features adequately to assist greatly in the identification and interpretation of such contributions.

However, of greater importance is the characterization of the fade duration distribution to a sufficient degree to permit development of a prediction procedure for the duration distribution that is associated with rain attenuation. Although the analysis has not yet proceeded to this level, it appears to be promising in this regard. Additional steps will be required to link the statistics of rain fading durations to the cumulative fade distribution, and to identify and partition the population of durations among the several individual contributions to the overall distribution. Of course, adjustments may be required to remove or account for durations that are attributed to equipment artifacts or other nonpath signal loss mechanisms. The techniques described in this paper to resolve individual contributions with exponential distributions indicate that partition of the loss mechanisms into identifiable populations is feasible.

This work is continuing with the goal of developing procedures to predict rain attenuation duration distributions for general conditions and locations.

### ACKNOWLEDGMENT

The authors express appreciation to Dr. C. Amaya and Mr. N. Reed for assistance in the conduct of this investigation, and to the Spectrum Engineering Directorate of Industry Canada, and in particular Mr. M. Gaudreau, for support.

### REFERENCES

1. ITU-T Recommendation G.821, "Error performance of an international digital connection forming part of an integrated services digital network," International Telecommunications Union, Geneva, 1980.
2. ITU-T Recommendation G.826, "Error performance parameters and objectives for international, constant bit rate digital paths at or above the primary rate," International Telecommunications Union, Geneva, 1994.
3. G. Brussaard, "Extreme-Value Analysis of Outage Durations due to Rain in Satellite Communication Systems," *Proc. 7<sup>th</sup> URSI Commission F Open Symposium*, pp. 13-16, Ahmedabad, India, 20-24 November 1995.
4. R. Lekkla, S.L. Lim, J. Wachja and K.S. McCormick, "Rain Attenuation Measurements in South-east Asia," *Proc. 7<sup>th</sup> URSI Commission F Open Symposium*, pp. 241-244, Ahmedabad, India, 20-24 November 1995.
5. R. Lekkla, K.S. McCormick and D.V. Rogers, "12-GHz Fade Duration Statistics on Earth-Space Paths in South-East Asia," *Proc. URSI Commission F Open Symposium on Climatic Parameters in Radiowave Propagation Prediction*, pp. 167-170, Ottawa, Canada, 27-29 April 1998.
6. R.K. Crane, X. Wang, D.B. Westenhaver and W.J. Vogel, "ACTS Propagation Experiment: Experiment Design, Calibration, and Data Preparation and Archival," *Proc. IEEE*, vol. 85, no. 6, pp. 863-878, June 1997.
7. R.K. Crane and D.V. Rogers, "Review of the Advanced Communications Technology Satellite (ACTS) Propagation Campaign in North America," *IEEE Antennas & Propagation Magazine*, vol. 40, no. 6, pp. 23-28, December 1998.

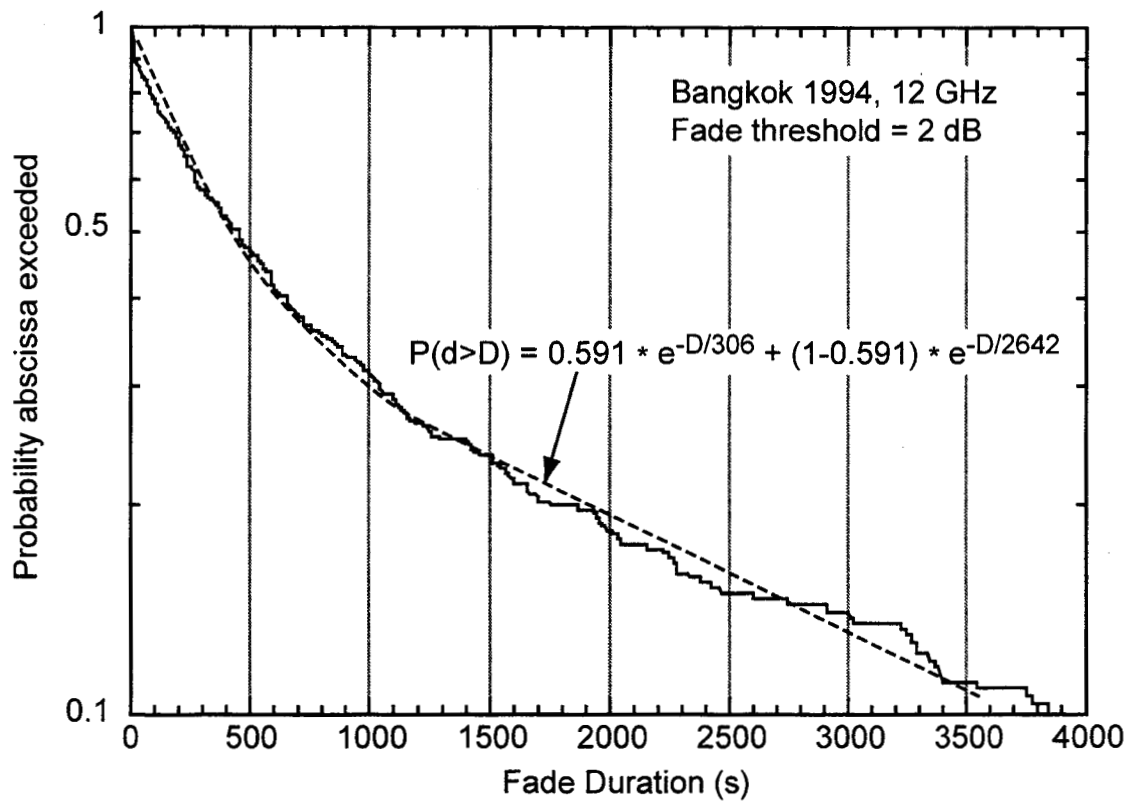


Figure 1. Fade duration distribution derived from 12 GHz radiometric measurements at Bangkok, 1994.

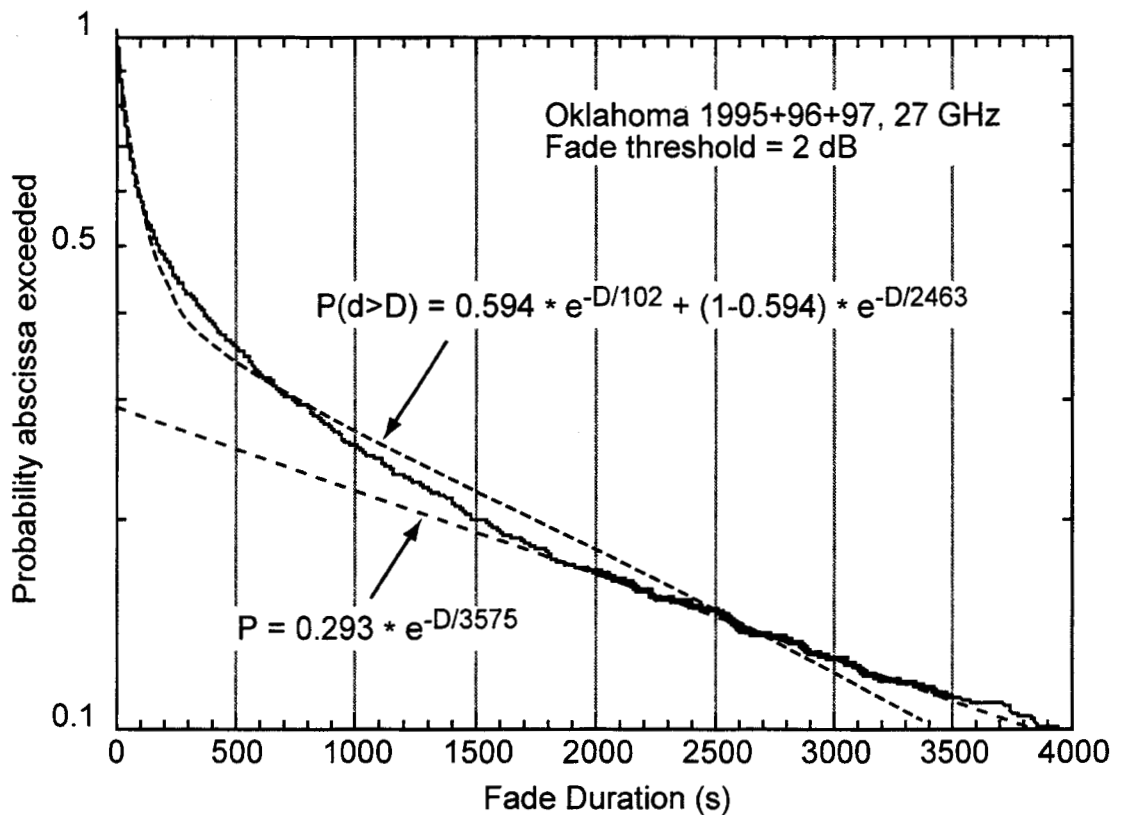


Figure 2. Fade duration distribution derived from the 27 GHz ACTS radiometer data for Oklahoma. Data were combined for the years 1995, 1996 and 1997.

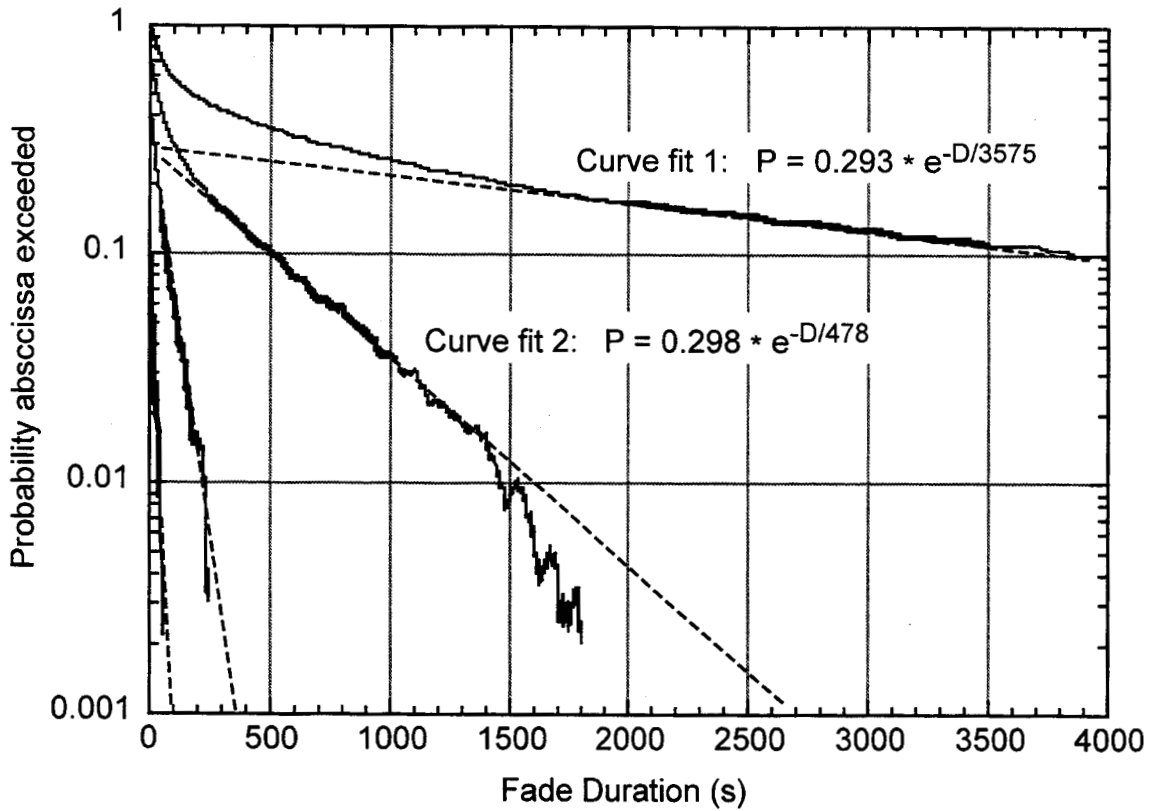


Figure 3. Curve fitting for the data of Figure 2. See text.

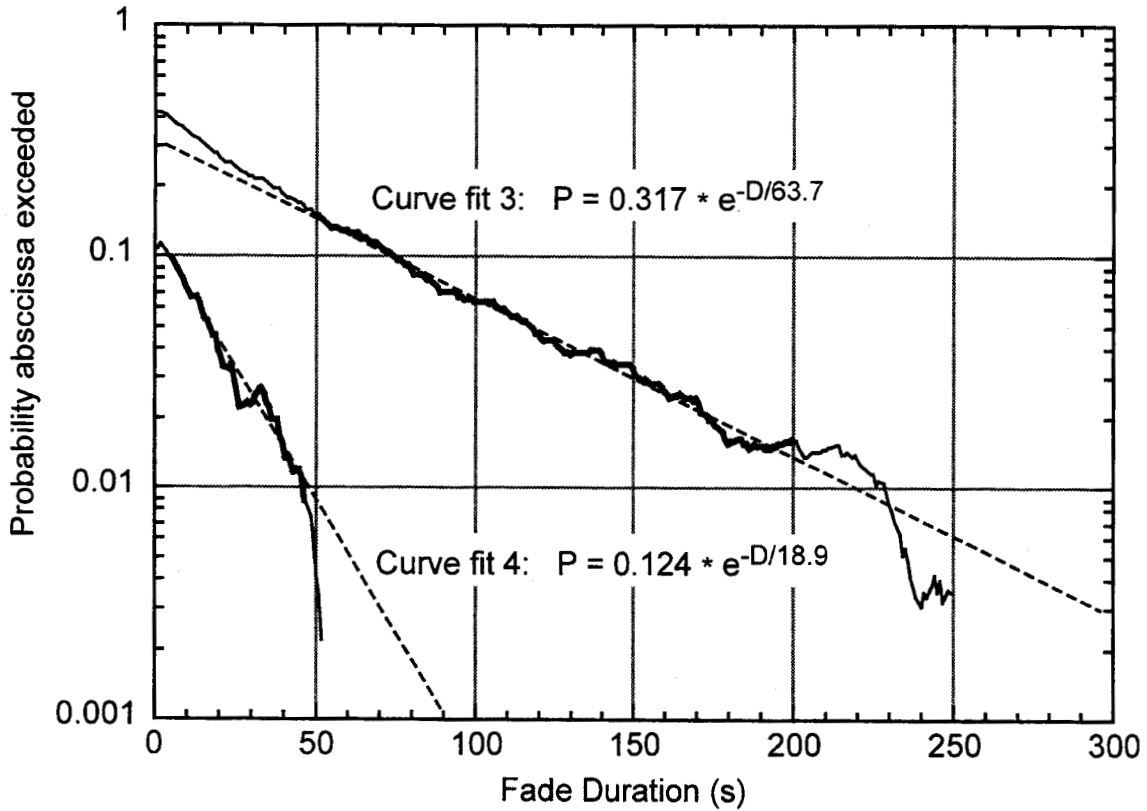


Figure 4. Curve fitting for the data of Figures 2 and 3. See text.

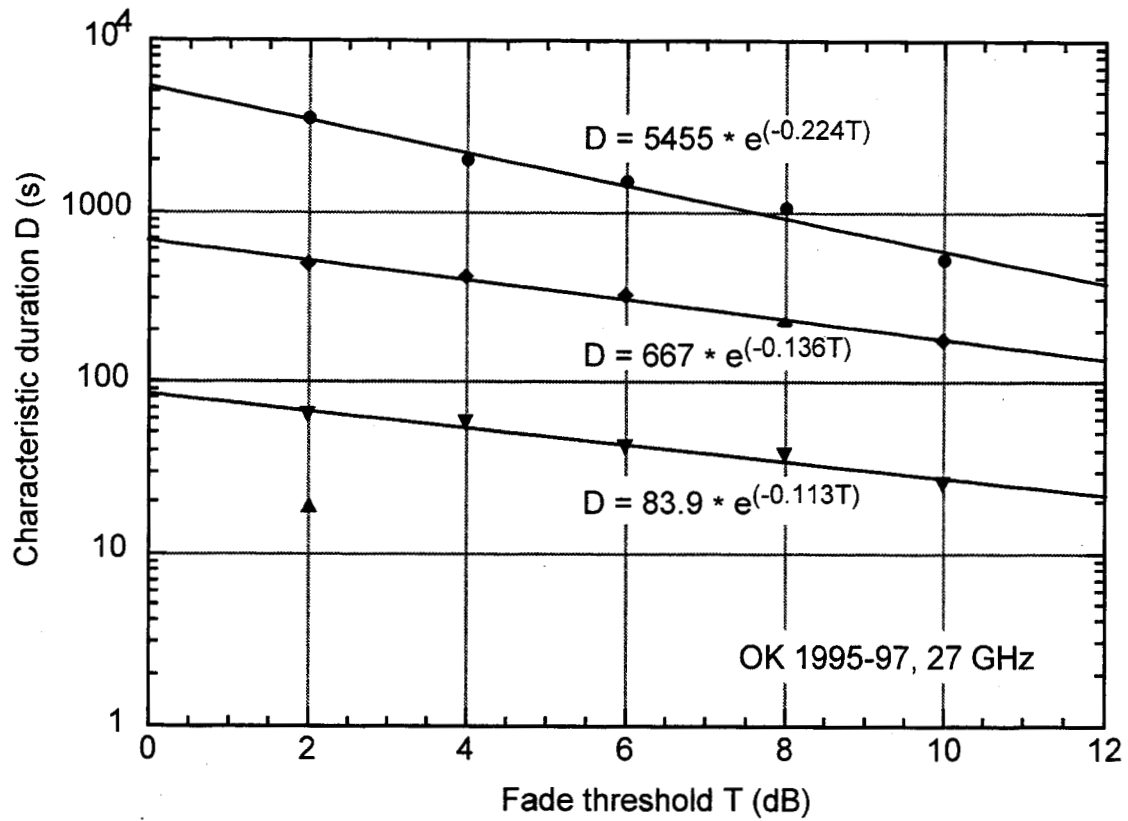


Figure 5. Characteristic durations derived from the Oklahoma data at 27 GHz as a function of fade threshold.

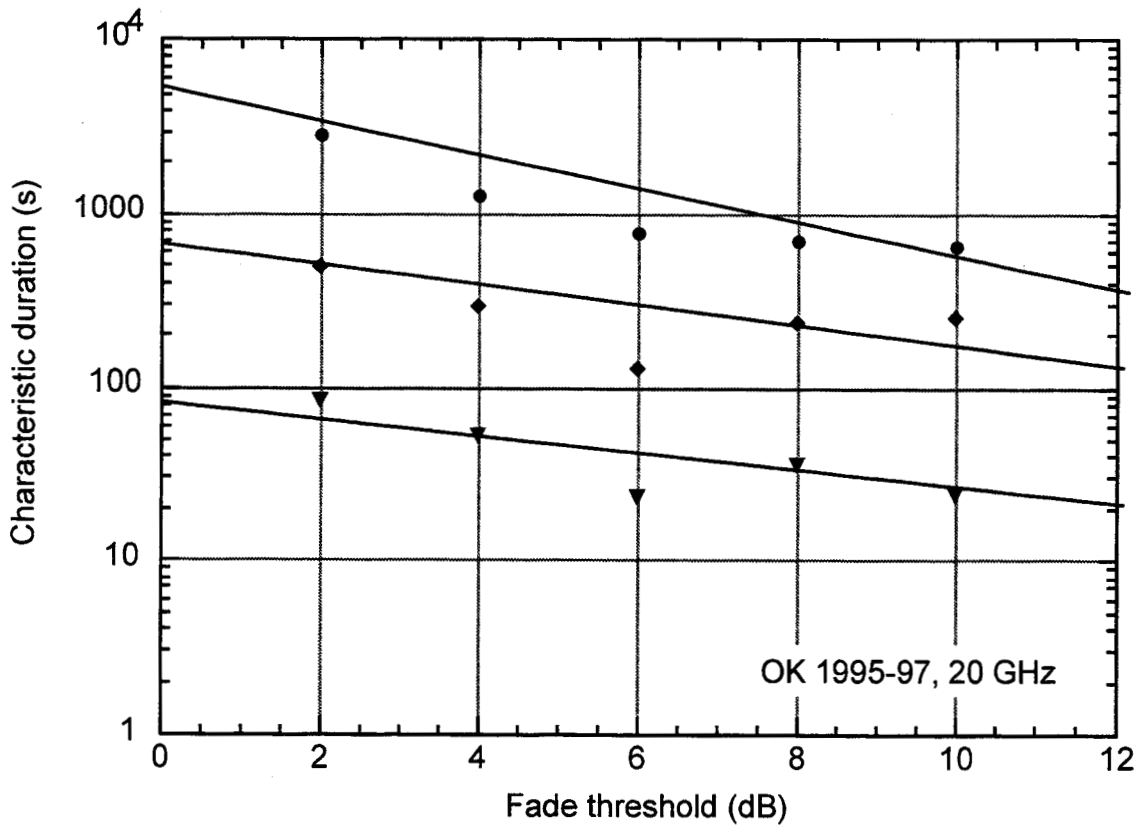


Figure 6. Characteristic durations derived from the Oklahoma data at 27 GHz as a function of fade threshold.

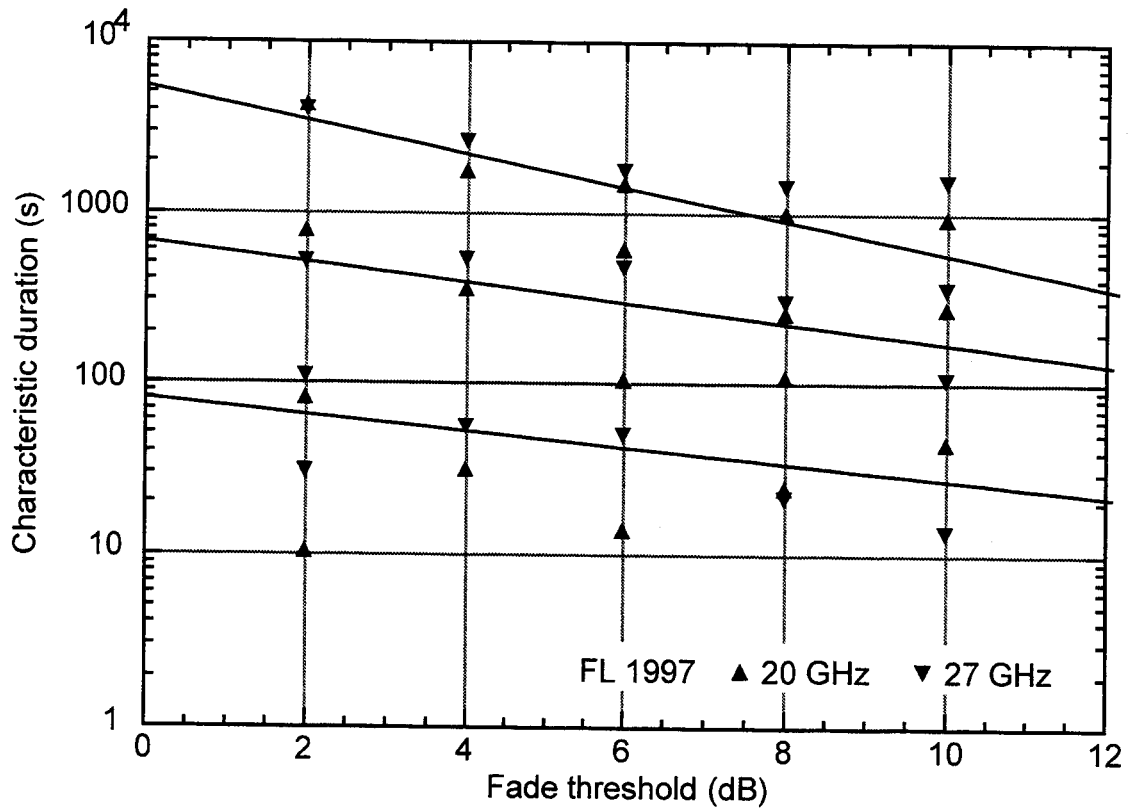


Figure 7. Characteristic durations derived from the Florida data at 20 and 27 GHz as a function of fade threshold.

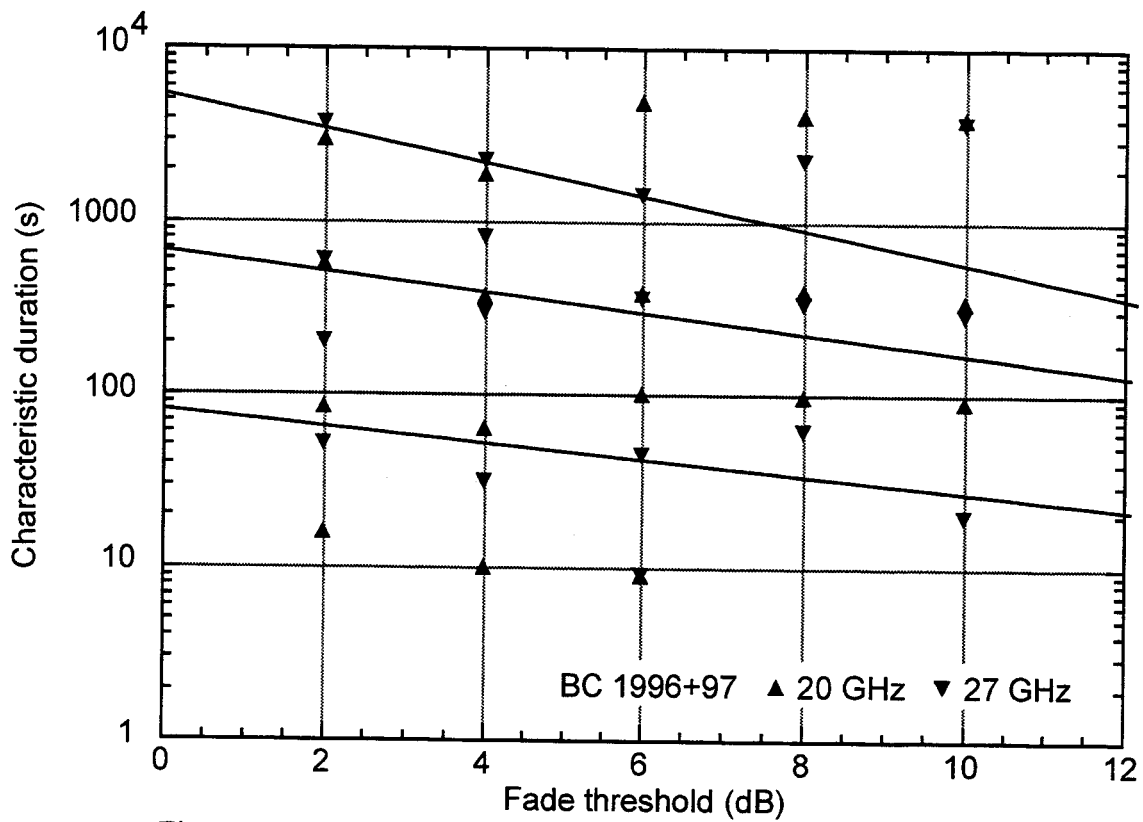


Figure 8. Characteristic durations derived from the Vancouver data at 20 and 27 GHz as a function of fade threshold.

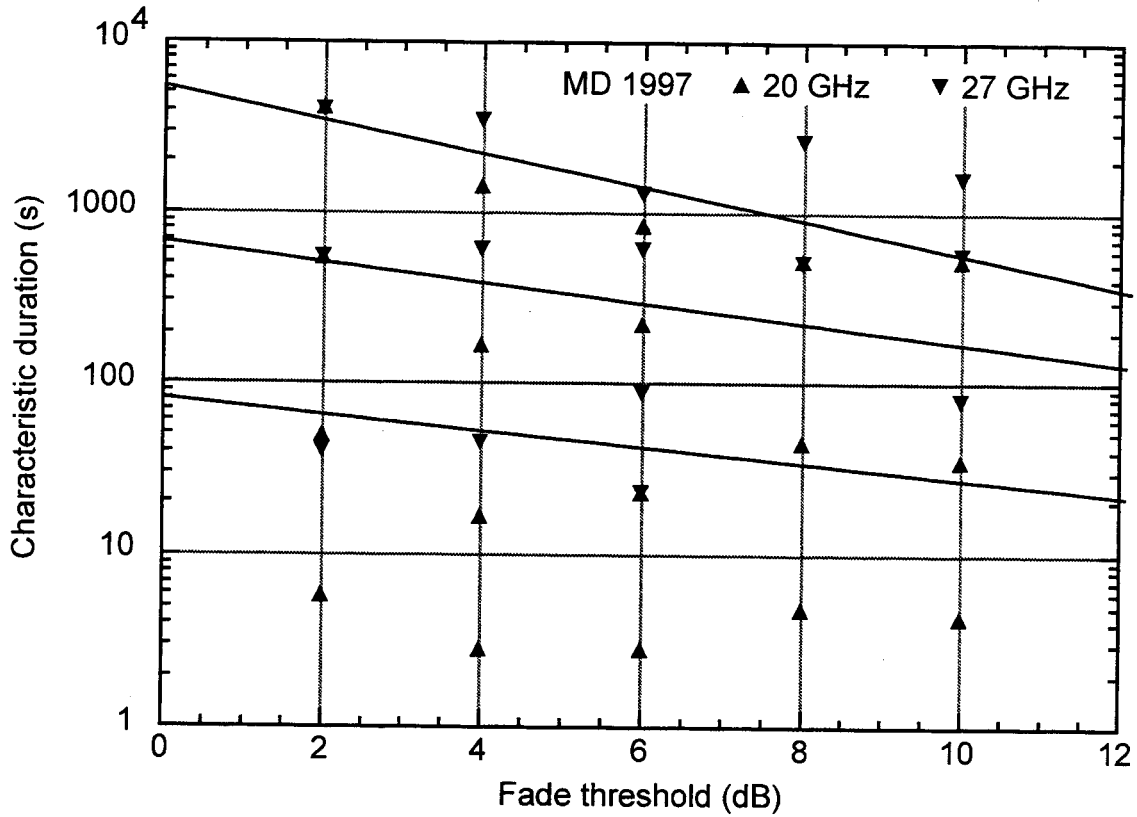


Figure 9. Characteristic durations derived from the Maryland data at 27 GHz as a function of fade threshold.

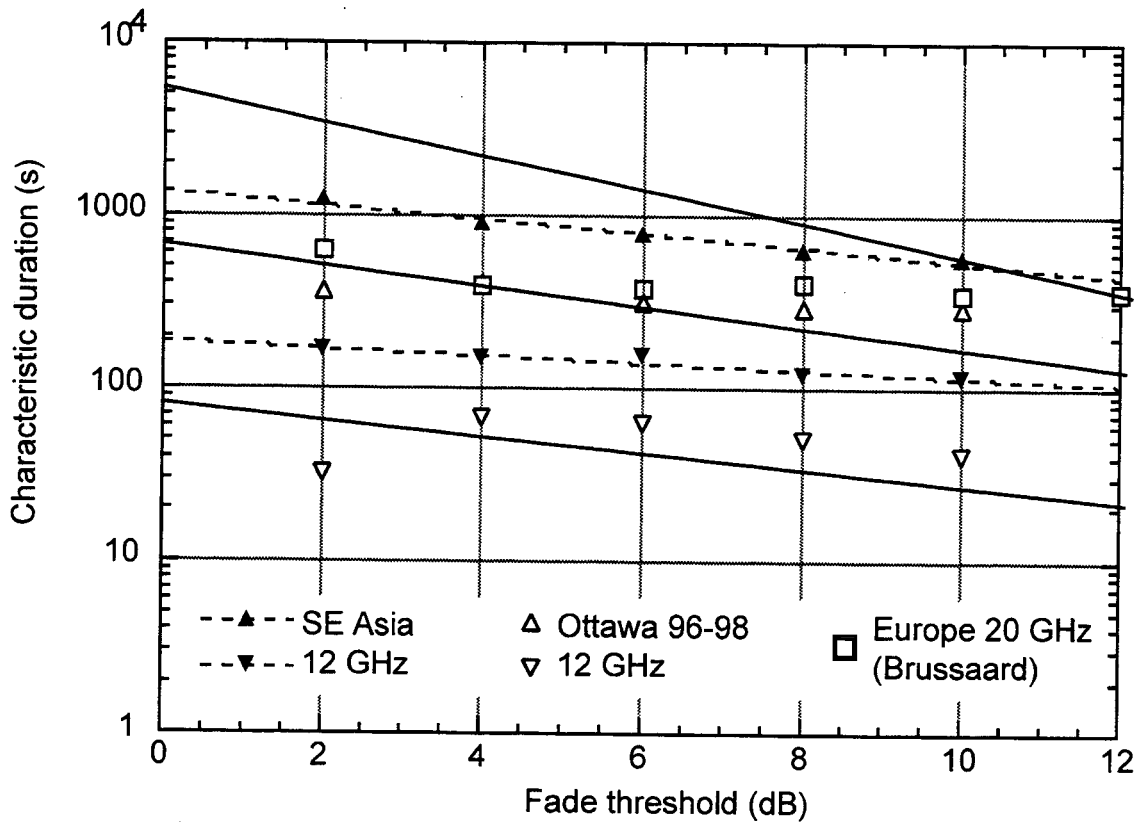


Figure 10. Characteristic durations derived for various locations and frequencies.